Working principles of the energy measurement system at BEPC Ⅱ *

MO Xiao-Hu(莫晓虎)[1;1)] FU Cheng-Dong(傅成栋)[2] ZHANG Jian-Yong(张建勇)[1] QIN Qing(秦庆)[1]
QU Hua-Min(屈化民)[1] WANG Yi-Fang(王贻芳)[1] XU Jin-Qiang(徐金强)[1] ZHANG Tian-Bao(张天保)[1]

1 (Institute of High Energy Physics, CAS, Beijing 100049, China)
2 (Tsinghua University, Beijing 100084, China)

Abstract The proposed beam energy measurement system at BEPC Ⅱ is composed of three parts: the laser source and optics system, the laser-electron interaction system and the HPGe detector system. The working principles of each system are expounded together with the calculation for preliminary design. The normalizations of laser and electron beams are put forth and used for the evaluation of intensity of the backscattering photon. The simulation of HPGe detector is also performed for understanding the working properties.

Key words energy measurement system, laser, electron, HPGe detector

PACS 29.00.00, 29.30.Kv, 78.40.Fy

1 Introduction

The large data sample to be collected at BESIII is typically a few fb^{-1}[1;2)], unprecedented statistical precision will be achieved in data analysis, hence many systematic factors and effects have to be considered seriously in order to obtain comparable correctness with precision. As pointed out in Ref. [2] the uncertainty of the beam energy plays an important role for BESIII physics analysis in many aspects. First of all, the detailed Monte Carlo simulation indicates[3, 4] that the uncertainty due to the beam energy will be the bottleneck issue for the accuracy improvement of τ mass measurement. Second, such kind of uncertainty is the crucial part for the further high accurate measurement of resonance parameters at BESIII. Last, small systematic uncertainty of the beam energy is also an independent factor for the improvement of branching ratio measurement aiming at the accuracy of 1%—2%.

Therefore, it is proposed to adopted the technique based on the Compton backscattering principle to directly measure the beam energy accurately[3)]. The detection system is determined to be allocated at the north interaction point (IP) of the storage ring[4)] as shown in Fig. 1 and Fig. 2.

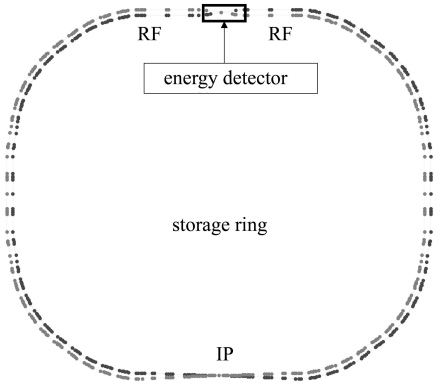

Fig. 1. Scheme of BEPCII storage ring. The interaction point (IP) is located at the south cross point of the storage ring while the energy measurement system is allocated at the north.

The proposed beam energy measurement system

Received 10 March 2008, Revised 4 August 2008

* Supported by National Natural Science Foundation of China (10491303, 10775412, 10775077, 10225522), Research and Development Project of Important Scientific Equipment of CAS (H7292330S7) and 100 Talents Programme of CAS (U-25)

1) E-mail: moxh@ihep.ac.cn

2) BESIII Collaboration, The BESIII Detector (January, 2004), IHEP-BEPCII-SB-13, internal report.

3) MO Xiao-Hu, "High accuracy energy measurement system for electron in storage ring", fund application report (2007.8.14).

4) Preliminary Design Report of accelerator BEPC Ⅱ (Second version, in Chinese; July, 2003), internal report.

(shortened as energy detector in Fig. 1) is composed of the following parts (classified for easy understanding of the general mechanism of the whole system):

1) Laser source and optics system;

2) Interaction region where the laser beam collides with the electron or positron beam;

3) High purity Germanium detector (HPGe) to measure the backscattering high energy γ-rays or X-rays.

In the following studies, we will describe each system. In the end, the energy measured at the north IP should be corrected for the synchrotron radiation, which is at level of 200 keV, and the corresponding error is less than 10% or equivalently 20 keV.

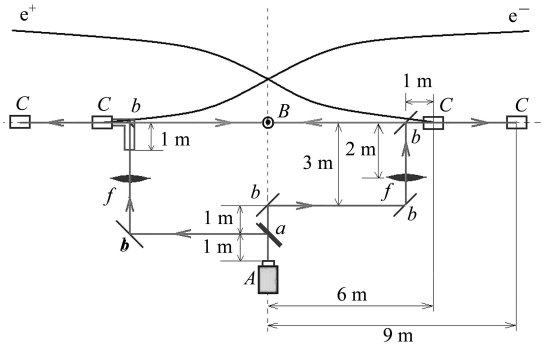

Fig. 2. The principle layout of energy measurement system. Two long curves denote the positron and electron projectiles. The bottle-like box (A) indicates the laser source; the circled dot (B) indicates the HPGe detector; rectangles (C) denote magnets; a indicates a half-transmission and half-reflection lens; b's indicate reflective lens and f's the focusing lens.

2 Laser and optics system

2.1 Laser beam

The electric field distribution of the fundamental mode (TEM_{00}) of oscillation of a stable cavity is a Gaussian. Without losing generality, we start from the TEM_{00} mode Gaussian beam, where TEM is the abbreviation for transverse electric and magnetic wave. The amplitude of this mode reads[5—7]

$$E(x,y,z)=E_0\cdot\frac{\sigma_0}{\sigma(z)}\mathrm{e}^{-\frac{x^2+y^2}{\sigma^2(z)}}\mathrm{e}^{-\mathrm{i}\left\{k\left[z+\frac{x^2+y^2}{R(z)}\right]-\tan^{-1}\frac{z}{f}\right\}}\ , \tag{1}$$

where

$$\sigma(z)=\sigma_0\sqrt{1+\left(\frac{z}{f}\right)^2}\ , \tag{2}$$

$$R(z)=z\left[1+\left(\frac{f}{z}\right)^2\right]\ , \tag{3}$$

with

$$f=\frac{\pi\sigma_0^2}{\lambda},\quad \sigma_0=\sqrt{\frac{\lambda f}{\pi}}\ . \tag{4}$$

In the above expressions, $k\equiv 2\pi/\lambda$; $\sigma(z)$ describes how the "beam width" varies with the distance along the axis of propagation. The beam has a minimum width at $z=0$ where $\sigma(0)$ is denoted as σ_0 and referred to as the "beam waist". $R(z)$ indicates the radius of curvature at the interaction point of the wave front with the z axis. f is the confocal parameter, and according to Eq. (2) it denotes the distance from the beam waist in which the beam spot size increases by $\sqrt{2}$ and is a convenient measure of the convergence of the input beam.

In the light of Eq. (1), the beam parameters $\sigma(z)$ and $R(z)$ completely specify the geometry of a Gaussian beam, then it can be readily to calculate the field at any point (x,y,z) in a radiation beam of wave length λ and amplitude E_0. Usually, it is more convenient to introduce a complex beam parameter

$$\frac{1}{q(z)}=\frac{1}{R(z)}-\mathrm{i}\frac{\lambda}{\pi\sigma^2(z)}\ , \tag{5}$$

with it, Eq. (1) is recasted as

$$E(x,y,z)=E_0\cdot\frac{\sigma_0}{\sigma(z)}\mathrm{e}^{-\mathrm{i}k\left[\frac{x^2+y^2}{2q(z)}\right]}\mathrm{e}^{-\mathrm{i}\left(kz-\tan^{-1}\frac{z}{f}\right)}\ , \tag{6}$$

and

$$\frac{1}{R(z)}=\mathcal{R}\left[\frac{1}{q(z)}\right],\quad \frac{1}{\sigma^2(z)}=\frac{\pi}{\lambda}\cdot\Im\left[\frac{1}{q(z)}\right]\ . \tag{7}$$

It is found to be a useful substitution with q playing for the Gaussian wave, a role similar to that of the radius of curvature of a spherical wave. Sometimes q is called the complex radius of curvature.

With the help of the complex parameter q, the effect of the optical system on a laser beam can be expressed through the well-known $ABCD$ law[8] as follows

$$q_2=\frac{Aq_1+B}{Cq_1+D}\ , \tag{8}$$

where A, B, C, and D are components of transfer matrix for the particular optical system considered[1)].

1) Here the parameters A, B, C, and D indicate the feature of the medium passed through by the laser beam and they can be obtained by analyzing the character of the medium, as shown in Refs. [9, 10]. So far as Eq. (8) is concerned, it is actually the analogue of the formula

$$R_2=\frac{AR_1+B}{CR_1+D}$$

in classical optics, where R is the radius of curvature of the spherical wave. Formally speaking, the function of q for the laser beam is just as that of R for the spherical wave.

For example,

$$\begin{pmatrix} A & B \\ C & D \end{pmatrix} = \begin{pmatrix} 1 & 0 \\ -1/F & 1 \end{pmatrix}$$

is the transfer matrix for a laser beam passing through a thin lens whose input and output planes coincide. Another example is

$$\begin{pmatrix} A & B \\ C & D \end{pmatrix} = \begin{pmatrix} 1 & L \\ 0 & 1 \end{pmatrix},$$

which indicates the transfer matrix for a laser beam traveling a distance L between two planes in a homogeneous medium.

2.2 Optics system design

For our energy measurement system, before the laser enters the storage ring, the beam should be focused in order to realize the effective collision between the laser and electron beams. As a simplified version, the principle drawing of our optics system is displayed in Fig. 3, assuming that the beam waist of the incident Gaussian beam is σ_0 (which should be accommodated by laser equipment), the distance between the waist and lens is l, with the focal length F for lens. Here the location (l') and magnitude (σ_0') of the waist of the output beam should be figured out.

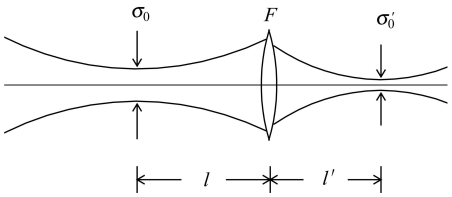

Fig. 3. The transformation of a Gaussian beam by the lens with the focal length F. σ_0 and σ_0' denote the waists of laser beam before and after passing through the len; l (l') is the corresponding distance between σ_0 (σ_0') and the lens.

Denote the parameter of the input Gaussian beam at the waist as $q_1 = q(z_1)$, and that of the output Gaussian beam at the waist as $q_2 = q(z_2)$, viz.

$$\begin{cases} q_1 = \mathrm{i}f \ , \\ q_2 = \mathrm{i}f' \ . \end{cases} \tag{9}$$

The transformation from the input waist position to the output waist position include: free propagation with the distance l, pass-through lens with focal length F, and free propagation with the distance l'. The corresponding transform matrixes denoted as M_l, M_F, $M_{l'}$, and the synthetic transformation matrix is

$$\begin{aligned} M \ &= \ M_{l'} M_F M_l = \\ &\begin{pmatrix} 1 & l' \\ 0 & 1 \end{pmatrix} \begin{pmatrix} 1 & 0 \\ -\dfrac{1}{F} & 1 \end{pmatrix} \begin{pmatrix} 1 & l \\ 0 & 1 \end{pmatrix} = \\ &\begin{pmatrix} 1-\dfrac{l'}{F} & \dfrac{Fl'+Fl-ll'}{F} \\ -\dfrac{1}{F} & 1-\dfrac{l}{F} \end{pmatrix} \ . \end{aligned} \tag{10}$$

By virtue of the $ABCD$ law, it is obtained

$$\mathrm{i}f' = \frac{\left(1-\dfrac{l'}{F}\right)(\mathrm{i}f) + \dfrac{Fl'+Fl-ll'}{F}}{\left(-\dfrac{1}{F}\right)(\mathrm{i}f) + \left(1-\dfrac{l}{F}\right)} \ . \tag{11}$$

Equalizing the real and imaginary parts of the above equation leads to

$$f' = \frac{F^2 f}{(l-F)^2 + f^2} \ , \tag{12}$$

$$l' = \frac{l(l-F)+f^2}{(l-F)^2+f^2} \cdot F \ . \tag{13}$$

Utilizing the relation given in Eq. (4), Eq. (12) can be rewritten as

$$\sigma_0' = \frac{F}{(l-F)^2 + \pi^2 \sigma_0^4 / \lambda^2} \cdot \sigma_0 \ . \tag{14}$$

The immediate application of the above calculation is the design of optics system for laser transformation. In the design, the f (equivalently σ_0) is determined by laser instrument, f' should satisfy the intensity requirement for collision between the laser and electron beams; and l' should be long enough after taking into account the construction of vacuum tube at north IP. So the problem becomes finding the suitable values of l and F with the known quantities f, f', and l'. Starting from Eq. (11) and expressing l and F as the functions of f, f', and l', we have

$$l^2 = \frac{f}{f'} \cdot [(l')^2 + (f')^2] - f^2 \ , \tag{15}$$

$$F = \frac{l'f - f'l}{f - f'} \ . \tag{16}$$

As a suggestive design, the beam waist is assumed to be 2 m[11], the beam waist is required to be 1.5 mm at IP; and the distance between the IP and the converging lens is 6 m. With these input values and by virtue of Eqs. (15) and (16), it is obtained $F = 3.48$ m and $l = 7.96$ m. The corresponding design plot is shown in Fig. 2.

2.3 Beam normalization

The last question we want to discuss in this section is the normalization of laser beam. Rewriting

Eq. (1) as follows

$$\psi(x,y,z)=C\cdot\exp\left[-\frac{x^2+y^2}{\sigma^2(z)}\right]\cdot\exp\left[\mathrm{i}\theta(x,y,z)\right] \ . \quad (17)$$

Here $\psi(x,y,z)$ denotes the amplitude of the TEM_{00} mode Gaussian beam; the phase factor is simplified as $\theta(x,y,z)$, which has no effect on the following discussion; C is the constant to be determined below. With Eq. (17), we obtain the photon density of laser beam

$$\rho_\gamma=|\psi(x,y,z)|^2=\rho_0\cdot f_\gamma(x,y,z), \quad (18)$$

$$f_\gamma(x,y,z)=\exp\left[-\frac{2(x^2+y^2)}{\sigma^2(z)}\right] \ . \quad (19)$$

To determine the constant $\rho_0=C^2$ in Eq. (19), we consider the differential relation between the laser power (P) and photon density:

$$\mathrm{d}P=\omega_\gamma\cdot\rho_\gamma\cdot\Delta S\cdot c \ , \quad (20)$$

where ω_γ is the energy of laser beam, c the velocity of light, and ΔS the intersection area passed through by the laser beam. The integral of the above relation gives:

$$P=\rho_0\cdot(\omega_\gamma\cdot c\cdot\pi\cdot\sigma^2(z)/2) \ ,$$

or

$$\rho_0=\frac{2P}{\omega_\gamma\cdot c\cdot\pi\cdot\sigma^2(z)} \ . \quad (21)$$

From dimensional analysis, we notice that ρ_0 has dimension of inverse volume, so the photon density ρ_γ is actually the volume density distribution.

3 Electron beam and interaction

3.1 Electron beam

Analogously, for the electron (positive or negative) beam, the density function can be simplified as follows[12, 13]

$$\rho_\mathrm{e}=\rho_0'\cdot f_\mathrm{e}(x,y,z), \quad f_\mathrm{e}(x,y,z)=\exp\left[-\left(\frac{x^2}{\sigma_x^2}+\frac{y^2}{\sigma_y^2}\right)\right], \quad (22)$$

where σ_x and σ_y are the standard deviations of electron beam in x and y directions, respectively; ρ_0' is the normalization factor which is determined by the differential relation between the current intensity (I) and electron density:

$$\mathrm{d}I=e\cdot\rho_\mathrm{e}\cdot\Delta S\cdot u_\mathrm{e} \ , \quad (23)$$

where e is the electron charge, u_e the velocity of electron beam, and ΔS the intersection area passed through by the electron beam. The integral of the above relation gives:

$$P=\rho_0'\cdot(u_\mathrm{e}\cdot e\cdot 2\pi\cdot\sigma_x\sigma_y) \ ,$$

or

$$\rho_0'=\frac{I}{u_\mathrm{e}\cdot e\cdot 2\pi\cdot\sigma_x\sigma_y} \ . \quad (24)$$

From dimensional analysis, we notice that ρ_0' has dimension of inverse volume, so the electron density ρ_e is actually the volume density distribution.

3.2 Compton backscattering principle

The interaction of electron and laser beam is depicted by the Compton backscattering principle[14, 15]. The energy of the scattering photon (ω_2) reads

$$\omega_2=\frac{\omega_1(1-\beta\cos\phi_1)}{1-\beta\cos\phi_2+\dfrac{\omega_1}{\gamma m}(1-\cos[\phi_1-\phi_2])} \ . \quad (25)$$

With Eq. (25) we can calculated the various dependence of ω_2 on the injection laser beam (ω_1), the electron energy (E_e, notice $\beta=\sqrt{E_\mathrm{e}^2-m_\mathrm{e}^2}/E_\mathrm{e}$ and $\gamma=E_\mathrm{e}/m_\mathrm{e}$), the observation angle (ϕ_2) or the injection angle (ϕ_1). Fig. 4 shows the dependence of the energy of backscattering photons on the electron energy and injection energy of the laser beam, respectively. From Fig. 4(a), it can be seen for the

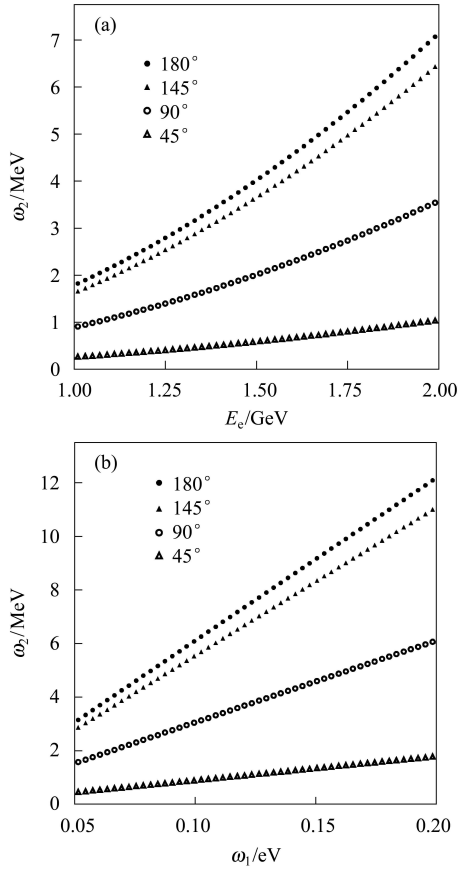

Fig. 4. Variation of the energy of backscattering photons with (a) electron energy and (b) injection laser energy. (a) Fixed observation angle $\phi_2=0^\circ$ and $\omega_1=0.117$ eV; (b) Fixed observation angle $\phi_2=0^\circ$ and $E_\mathrm{e}=2$ GeV.

BEPCII designed energy region (1 to 2 GeV), the corresponding energy range for the head-on backscattering photon is around 2 to 7 MeV.

Next we consider cross section. When the unpolarized light is scattered from the unpolarized electrons and neither the spin of the residual electron nor the polarization of the final photon are observed, the differential cross section in terms of the relativistic invariants is obtained as[15]

$$\frac{\mathrm{d}\sigma}{\mathrm{d}t}=2\pi r_{\mathrm{e}}^2\frac{1}{(mx_1)^2}\left\{4y(1+y)-\frac{x_1}{x_2}-\frac{x_2}{x_1}\right\}\ , \quad (26)$$

where r_{e} is the classical electron radius[16] and

$$x_1 = 2\gamma\frac{\omega_1}{m}(1-\beta\cos\phi_1)\ , \quad (27)$$

$$x_2 = -2\gamma\frac{\omega_2}{m}(1-\beta\cos\phi_2)\ , \quad (28)$$

$$y = \frac{1}{x_1}+\frac{1}{x_2}\ . \quad (29)$$

In a scattering experiment x_1 is fixed by the energies of the initial electron and photon. The total cross section is obtained by integrating over x_2 at the fixed value of x_1 (see e.g. Ref. [15])

$$\sigma = 2\pi r_{\mathrm{e}}^2\frac{1}{x_1}\left\{\left(1-\frac{4}{x_1}-\frac{8}{x_1^2}\right)\ln(1+x_1)+\frac{1}{2}+\frac{8}{x_1}-\frac{1}{2(1+x_1)^2}\right\}\ . \quad (30)$$

When observed in the laboratory, however, the Lorentz transformation concentrates the photon flux at small angle ϕ_2 of the order of $1/\gamma$, increasing therefore the photon flux at forward angles. By virtue of Ref. [17], the differential cross section per unit solid angle can be expressed as follows

$$\frac{\mathrm{d}\sigma}{\mathrm{d}\Omega}=2r_{\mathrm{e}}^2\left(\frac{\omega_2}{mx_1}\right)^2\left\{4y(1+y)-\frac{x_1}{x_2}-\frac{x_2}{x_1}\right\}\ . \quad (31)$$

The formulas of (30) and (31) will be used afterward to calculate the interaction cross section between the laser beam and the high energy electron beam. Fig. 5 shows the energy-integrated differential cross sections $\mathrm{d}\sigma/\mathrm{d}\Omega$ for Compton scattering of 0.117 eV photons from relativistic electrons with energy $E_{\mathrm{e}}=1776.99$ MeV (the beam energy at τ-lepton threshold[16]).

3.3 Interaction description

In the light of the descriptions of laser beam and electron beam in Sections 2.3 and 3.1 respectively, we calculate the intensity of backscattering photon. We start from a simplified interaction picture: the laser beam makes a "head-on" collision with the electron beam, the intensity of backscattering photon can be

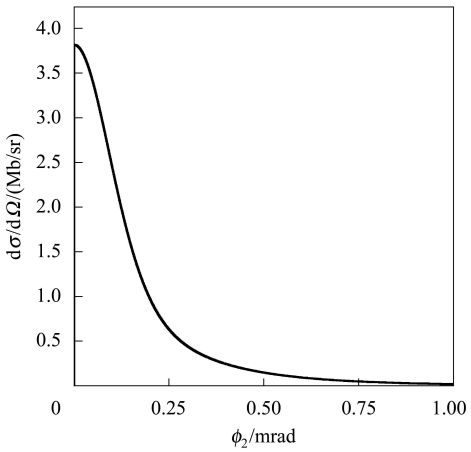

Fig. 5. Differential cross sections for Compton scattering of 0.117 eV photons from relativistic electrons at an incidence angle $\phi_1=180°$.

calculated by the formula:

$$N_\gamma = u_{\mathrm{e}}\sigma_{\mathrm{T}}\cdot\iiint\rho_\gamma\cdot\rho_{\mathrm{e}}\ \mathrm{d}x\mathrm{d}y\mathrm{d}z\ , \quad (32)$$

where ρ_γ (ρ_{e}) denotes the volume density of injection laser (electron) beam described by Eq. (19) and (21) (Eq. (22) and (24)); σ_{T} the total cross section accepted or detected by HPGe detector, can be evaluated by Eq. (31) (or approximately by Eq. (30)). More concretely, we could write the above equation as follows:

$$N_\gamma = \frac{PI\sigma_{\mathrm{T}}}{\omega_\gamma\cdot c\cdot e\cdot\pi^2}\iiint\frac{1}{\sigma^2(z)\sigma_x\sigma_y}f_\gamma\cdot f_{\mathrm{e}}\ \mathrm{d}x\mathrm{d}y\mathrm{d}z\ . \quad (33)$$

Using the parameters provided in Table 1 and by virtue of Eq. (33), we get

$$N_\gamma = 2.7\times10^8\ \mathrm{s}^{-1}\ .$$

Table 1. Some input parameters for the laser and electron beams.

laser beam	electron beam
power P=50 W	I=9.8 mA
wave-length λ=10. 59 μm	σ_x=1.6 mm
laser energy ω_γ=0.117 eV	σ_y=0.16 mm
waist radius r_0=2 mm	σ_z=15 mm

4 Detector system

4.1 HPGe detector

At BEPC Ⅱ the coaxial germanium detector (referred to as HPGe hereafter)[18] will be adopted, which is basically a cylinder of germanium with an n-type contact on the outer surface, and a p-type contact on the surface of an axial well[19]. The effective energy range of HPGe is from 50 keV to more than 10 MeV which is just satisfactory for the beam energy measurement at BEPC Ⅱ.

Germanium detectors are semiconductor diodes having a P-I-N structure in which the intrinsic region is sensitive to ionizing radiation, particularly X-rays and γ-rays. There are three types of reaction which happen in Germanium semiconductor, that is photoeffect, Compton scattering and pair production[20, 21] and the latter two processes dominate when the energy of injection photon is greater than 1 MeV. The germanium has a net impurity level of around 10^{10} atoms/cm^3 (an extremely small relative net impurity concentration compared to 4×10^{22} Ge atoms/cm^3[20]) so that with moderate reverse bias voltage, the intrinsic region that is the entire volume between the electrodes is depleted, and an electric field extends across this active region. When photons interact with the material within the depleted volume of a detector, charge carriers (holes and electrons) are produced and are swept by the electric field to the P and N electrodes. This charge, which is in proportion to the energy deposited in the detector by the incoming photon, is converted into a voltage pulse by an integral charge sensitive preamplifier. Subsequent amplification and pulse height analysis add the pulse to accumulated histogram which eventually becomes the characteristic spectrum of the source.

4.2 Simple simulation

Figure 6(a) shows a sketch of coaxial HPGe detector configuration. To understand the working feature,

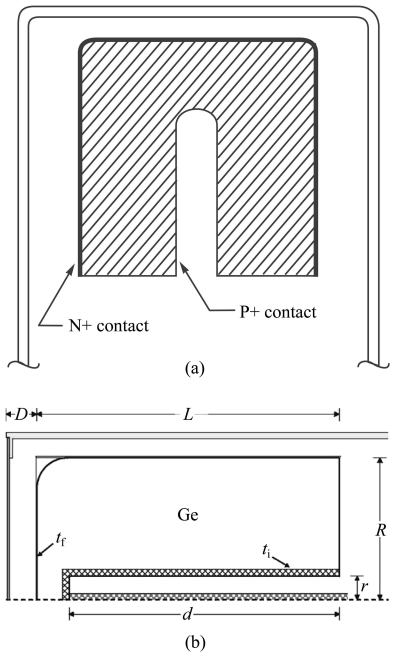

Fig. 6. (a) Sketch of coaxial HPGe detector configuration; (b) Sectional view of one-half a detector, which has cylindrical symmetry about the marked center line. Dimensions given in Table 1 are identified by the same letters in the figure.

we simulate the HPGe detection on injection photon with energy $E=5$ MeV. The parameters of HPGe[22] used in simulation are listed in Table 2 (also refer to Fig. 6(b)) and GEANT4 package [23] is used for the simulation.

Table 2. Properties of HPGe detector in simulation.

dimension	value nominal
crystal radius, R	35 mm
crystal length, L	80 mm
cap face to crystal distance, D	6 mm
hole radius, r	6 mm
hole depth, d	70 mm
thickness of internal (Li) dead layer, t_i	1 mm
thickness of front dead layer, t_f	0.3 mm

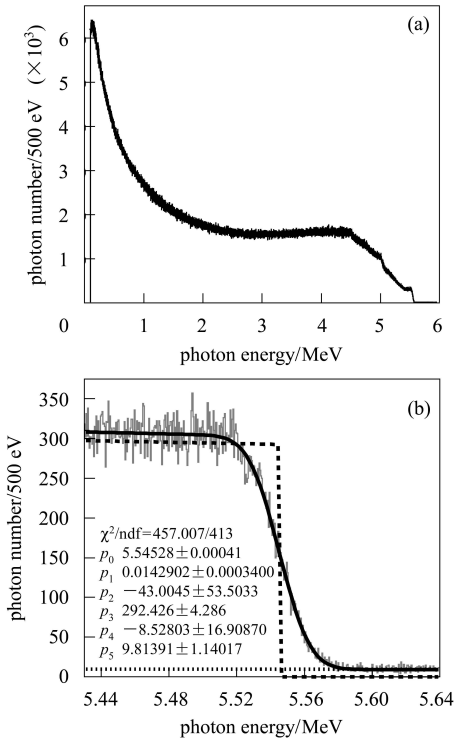

Fig. 7. Simulation of the received events by HPGe detector. (b) is the close-up of the spectrum of (a) around the edge at maximum energy of the scattering photons. The solid line indicates a fit through the spectrum, the dashed line illustrates the assumed line shape in the absence of the finite detector resolution and energy spread, and the dotted line denotes the background shape. (a) Simulation from 0 to 6 MeV; (b) Simulation from 5 to 5.7 MeV.

A small part of Compton spectrum of Fig. 7(a) around $\omega_2^{\max}$ is shown in Fig. 7(b). The pure sharp edge at $\omega_2^{\max}$ is approximated by the normalized function[24]

$$h(x)=[p_3+p_2(x-p_0)]\Theta(p_0-x)\ , \qquad (34)$$

with p_3 being the slope of the line before the edge. The product $p_2(x-p_0)$ is small compared to p_3; for

$p_2=0$ and $p_3=1$, $h(x)$ reduces to the normal step function. The function $h(x)$ is then folded with a Gaussian of standard deviation p_1

$$g(x)=\frac{1}{\sqrt{2\pi}p_1}\mathrm{e}^{-\frac{x^2}{2p_1^2}} \ . \tag{35}$$

The resulting function for variable position and height of the edge is given by

$$f(x)=\int_{-\infty}^{+\infty}\mathrm{d}t\,h(t)g(x-t) \ . \tag{36}$$

Anyway, due to the existence of background, a linear function $p_4(x-p_0)+p_5$ is added to $f(x)$ to describe the shape of background. Therefore the final synthetic function has the form[18]:

$$g(x,\boldsymbol{p}) = \frac{1}{2}(p_2(x-p_0)+p_3)\cdot\mathrm{erfc}\left[\frac{x-p_0}{\sqrt{2}p_1}\right]+ \frac{p_1p_2}{\sqrt{2\pi}}\cdot\exp\left[-\frac{(x-p_0)^2}{2p_1^2}\right]+p_4(x-p_0)+p_5 \ , \tag{37}$$

with[25]

$$\mathrm{erfc}(z)\equiv\frac{2}{\sqrt{\pi}}\int_z^\infty\mathrm{d}u\,\mathrm{e}^{-u^2}.$$

The parameters in Eq. (37) are: p_0 is edge position; p_1 is edge width; p_2 is slope left; p_3 is edge amplitude; p_4 is slope right; p_5 is background. Parameter p_0 gives the information about the average electron beam energy during the data acquisition period, while p_1 is mostly coupled with the electron beam energy spread.

5 Discussion

In this monograph, recapitulated are the working principles for three major subsystems of beam energy measurement system at BEPC Ⅱ, that is laser and optics subsystem, interaction subsystem, and HPGe detector subsystem. Targeting on our special case, two normalization schemes for laser and electron beams are presented and the principle design of optics system is figured out based on the ABCD law. In addition, the simple simulation based on GEAN4 package is performed and the preliminary results are obtained. All of these results, which represent the main parts and contain main features of a realistic system, are the bases for both further detailed study and practical engineering design.

Anyway, as we know there are a variety of actual factors and effects which should be taken into account in the work that follows. Some of them are listed as follows and will be tackled in the following study:

1) Laser and optics system

Due to spatial constraint, optical equipments such as focusing or reflecting lens, are needed to transfer the laser beam into the storage ring. So the effects of optics system on the beam strong and corresponding uncertainty for backscattering photon should be considered.

2) Electron and interaction system

The realistic electron beams have their own distributions both for position and energy. Moreover, for actual running, the electron beams have not only vertical but also horizontal deviations. All these will definitely affect the distribution of backscattering photon.

3) HPGe Detector system

Here the magnitude, efficiency, acceptance of HPGe conduct should be considered. Furthermore, the accuracy of calibration γ source also needs experimental measurements.

We would like to thank Drs. M. N. Achasov and N. Yu. Muchnoi for their friendly discussions. Thanks also go to Prof. A. Bondar who put forth a good suggestion for the design of energy measurement system at BEPC Ⅱ.

References

1 YUAN Chang-Zheng, ZHANG Bing-Yun, QIN Qing. HEP & NP, 2002, **26**: 1201—1208 (in Chinese)
2 FU Cheng-Dong, MO Xiao-Hu. Significance of Energy Scale for Physics at BESⅢ. China Phys. C, 2008, **32**: 776—780
3 MO Xiao-Hu. Nucl. Phys. B (Proc. Suppl.), 2007, **169**: 132—139
4 WANG You-Kai, MO Xiao-Hu, YUAN Chang-Zheng et al. Nucl. Instrum. Methods A, 2007, **583**: 479
5 Chang W S C. Principles of Lasers and Optics. Cambridge: Cambridge University Press, 2005
6 Yariv A. Quantum Electronics. New York: John Wiley & Sons, 1989
7 Maitland A, Dunn M H. Laser Physics. New York: John Wiley & Sons, 1969
8 Kogelnik H. Bell Syst. Tech. J, 1965, **44**: 455
9 YU K X et al. Pricinple of Laser and Technqiue of Laser. Beijing: Press of Beijing University of Technology, 2005 (in Chinese)
10 YAN J X et al. Pricinple and Technqiue of Laser. Beijing: Higher Education Press, 2004 (in Chinese)
11 The detailed and comprehensive introduction about laser products could be found through web page: http://www.coherent.com/Lasers/
12 JIN Y M. Physics of Electron Storage Ring. Revised Edition. Hefei: Press of University of Science and Technology of China, 2001 (in Chinese)
13 Lee S Y. Accelerator Physics. 2nd Edition. Shanghai: Fudan University Press, 2006
14 Rullhusen P, Artru X, Dhez P. Novel Radiation Sources Using Relativistic Electrons. Singapore: World Scientific

Publishing, 1998
15 Landau L D, Lifshitz E M. Relativistic Quantum Mechanics. Pergamon, 1971
16 YAO W M et al. Journal of Physics G, 2006, **33**: 1
17 Rauch J M, Rohrlich F. The Theory of Photons and Electrons. Addison-Wesley, 1959
18 Muchnoi N, Nikitin S, Zhilich V. Fast and Precise Beam Energy Monitor Based on the Compton Backscattering at the VEPP-4M Collider. EPAC-2006 report
19 The detailed and comprehensive introduction about HPGe products could be found through web page: http://www.canberra.com/products/
20 Haller E E. IEEE Transactions on Nuclear Science, 1982, **NS-29**: 1109
21 XIA Y F, NI X B, PENG Y Q. Applied Methods for Experimental Nuclear Physics. Beijing: Science Press, 1989 (in Chinese)
22 Hardy J C et al. Applied Radiation and Isotopes, 2002, **56**: 65
23 CERN Program Library Long Writeup W5013 for GEANT
24 Klein R et al. Nucl. Instrum. Methods A, 1997, **384**: 293
25 Gradshteyn I S, Ryzhik I M. Table of Integrals, Series, and Products. California: Elsevier Inc., 2007
26 Hagedorn R. Relativistic Kinematics. New York: W.A.Benjmain Inc., 1963

Appendix A
Kinematics of Compton Scattering

The interaction of electron and laser beam is depicted by the Compton backscattering principle[14, 15]. The kinematics of Compton scattering is determined by the 4-momentum conservation

$$p_1+k_1=p_2+k_2\ , \tag{A1}$$

and for relativistic energies it is convenient to describe the scattering process in terms of the relativistic invariants[26]

$$s = (p_1+k_1)^2=(p_2+k_2)^2\ , \tag{A2}$$
$$t = (p_2-p_1)^2=(k_1-k_2)^2\ , \tag{A3}$$
$$u = (p_1-k_2)^2=(p_2-k_1)^2\ , \tag{A4}$$

with

$$s+t+u=2m^2. \tag{A5}$$

In the laboratory these relativistic invariants are given in terms of the angles in the scattering geometry as depicted in Fig. A1:

$$s = m^2+2\gamma m\omega_1(1-\beta\cos\phi_1)\ , \tag{A6}$$
$$t = -2\omega_1\omega_2(1-\beta\cos\theta)\ , \tag{A7}$$
$$u = m^2-2\gamma m\omega_2(1-\beta\cos\phi_2)\ , \tag{A8}$$

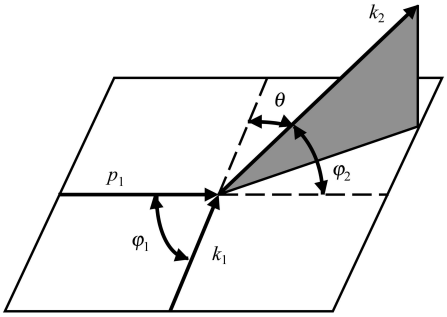

Fig. A1. Geometry of a Compton scattering experiment. The residual electron with momentum p_2 is not shown.

in which β and γm are the velocity and energy of the initial electron, respectively[1)]. Inserting (A6), (A7), and (A8) into (A5) one obtains for the energy ω_2 of the scattering photon

$$\omega_2=\frac{\omega_1(1-\beta\cos\phi_1)}{1-\beta\cos\phi_2+\dfrac{\omega_1}{\gamma m}(1-\cos\theta)}\ . \tag{A9}$$

If rescattering photon (k_2) is in the same plane determined by initial electron and laser beams (p_1 and k_2), then $\theta=\phi_1-\phi_2$ and Eq. (A9) becomes Eq. (25).

1) In high energy experiment, β and γ are often expressed as $\beta=p_1/E_1$ and $\gamma=E_1/m_{\rm e}$ ($m_{\rm e}$ electron mass), respectively.